

Primordial black hole dark matter from ultra-slow-roll inflation in Horndeski gravity

Despina Totolou,^{1,2,*} Theodoros Papanikolaou,^{3,4,2,†} and Emmanuel N. Saridakis^{2,5,6,‡}

¹*Department of Physics, Aristotle University of Thessaloniki, 54124 Thessaloniki, Greece*

²*Institute for Astronomy, Astrophysics, Space Applications and Remote Sensing,
National Observatory of Athens, 15236 Penteli, Greece*

³*Scuola Superiore Meridionale, Largo San Marcellino 10, 80138 Napoli, Italy*

⁴*Istituto Nazionale di Fisica Nucleare (INFN), Sezione di Napoli, Via Cinthia 21, 80126 Napoli, Italy*

⁵*Departamento de Matemáticas, Universidad Católica del Norte,
Avda. Angamos 0610, Casilla 1280 Antofagasta, Chile*

⁶*CAS Key Laboratory for Researches in Galaxies and Cosmology, Department of Astronomy,
University of Science and Technology of China, Hefei, Anhui 230026, P.R. China*

Primordial black holes (PBHs) provide a well-motivated non-particle candidate for dark matter, requiring an enhancement of curvature perturbations on small inflationary scales consistent with observational constraints. In this work we study PBH production within Horndeski gravity, accounting for compatibility with the GW170817 constraint on the gravitational-wave speed and imposing a constant coupling to the Ricci scalar. Under these conditions, and assuming an inflaton field characterised by a canonical kinetic term and a smooth potential, the inflationary dynamics is controlled by the cubic Horndeski interaction. We show that a suitable kinetic dependence of the latter enhances the effective friction acting on the inflaton, inducing a transient ultra-slow-roll phase embedded in an otherwise standard slow-roll evolution. Interestingly, this mechanism amplifies the curvature power spectrum on small scales without introducing any feature in the potential. For representative parameter choices we find that pronounced peaks in the scalar power spectrum are generated, leading to the formation of asteroid-mass PBHs with masses of order $\mathcal{O}(10^{-16}) M_\odot$, which can account for a substantial fraction of the dark matter abundance, reaching $f_{\text{PBH}} \simeq 0.9$, while satisfying current observational constraints. The resulting sharp features in the scalar power spectrum also imply potentially observable scalar-induced gravitational-wave signatures.

I. INTRODUCTION

According to recent cosmological observations by the Planck satellite, approximately 26% of the total energy budget of the Universe consists of dark matter (DM), interacting predominantly through gravity with ordinary baryonic matter [1]. Despite the remarkable success of the standard cosmological model in describing a wide range of observations, the physical nature and origin of dark matter remain unresolved. The majority of proposed DM candidates are rooted in extensions of particle physics beyond the Standard Model [2, 3], yet no conclusive experimental evidence for such particles has been established so far.

An alternative, non-particle candidate for dark matter is provided by primordial black holes (PBHs), which may have formed in the early Universe from the gravitational collapse of enhanced density fluctuations [4–6]. Depending on the epoch of their formation, PBHs can span a very wide mass range, from the Planck scale, i.e. $\sim 10^5$ g, up to supermassive values of $\mathcal{O}(10^{15} M_\odot)$. On the other hand, observational constraints on their abundance arise from a variety of probes, including the Cosmic Microwave Background (CMB), gravitational lensing, gravitational waves, accretion effects and large-scale

structure (LSS) formation [7–10]. Within certain mass windows, most notably at asteroid and sub-lunar masses, PBHs remain viable candidates that could account for a significant fraction, or even the totality, of the dark matter abundance.

PBH formation is commonly investigated in the context of inflation, where enhanced curvature perturbations on small scales may re-enter the horizon during radiation domination and collapse gravitationally. In order to produce a non-negligible PBH abundance, the curvature power spectrum must be amplified to values of order $\mathcal{O}(10^{-2})$ on scales far smaller than those directly constrained by CMB and LSS probes. Such enhancements may originate from specific features in the inflationary potential, including steps [11, 12], bumps or dips [13–15], or from waterfall fields in hybrid inflationary models [16, 17]. Another well-studied mechanism involves a transient phase of ultra-slow-roll (USR) inflation, during which the inflaton experiences additional friction and its velocity decreases rapidly [11, 18–20].

In conventional setups, the extra friction required to trigger the USR phase is typically generated either by an inflection point or a plateau in the inflationary potential [21–23], by non-canonical kinetic terms [24–26] or through explicit modifications of the friction term [27, 28]. In this work, we focus on the last possibility, considering USR inflation induced by modified friction of gravitational origin, while remaining within a single-field inflationary framework and avoiding the introduction of sharp features or discontinuities in an otherwise smooth inflationary potential.

*Electronic address: dtotolo@auth.gr

†Electronic address: t.papanikolaou@ssmeridionale.it

‡Electronic address: msaridak@phys.uoa.gr

Our motivation to work within modified gravity theories arises from both theoretical and phenomenological considerations [29]. From a theoretical perspective, modified gravity frameworks offer ways to address issues such as spacetime singularities and renormalizability issues that arise in general relativity [30, 31]. From an observational standpoint, modifications of gravity can effectively describe dark components of the Universe, including dark energy and dark matter, either through genuine gravitational degrees of freedom or through effective energy-momentum contributions [32, 33], and moreover can alleviate various cosmological tensions [34]. Among such classes, the Horndeski (or Generalized Galileon) gravity occupies a distinguished position, as it represents the most general scalar-tensor theory in four dimensions with a single scalar field, leading to second-order field equations and avoiding Ostrogradsky instabilities [35–37]. The explicit dependence of the Lagrangian on the canonical kinetic term of the scalar field makes this framework particularly relevant in describing inflationary and dark energy epochs [38–59].

Primordial black hole formation in Horndeski gravity has been explored in several recent works, mainly by engineering features in the inflationary potential $V(\phi)$ in order to induce a USR phase [60–62]. However, the observation of the binary neutron star merger GW170817 imposes stringent constraints on scalar-tensor theories, requiring the speed of gravitational waves to coincide with the speed of light at late times. This condition severely restricts the allowed Horndeski interactions, effectively excluding higher-order Galileon terms [63–65]. Within these GW170817-compatible Horndeski models, enhancements of the curvature power spectrum have so far been achieved mainly through suitable choices of the inflationary potential [66, 67] or through particular dependence of different Horndeski terms on the inflaton field ϕ [68].

In this paper, we depart from this standard approach. While maintaining a canonical kinetic term and a smooth inflationary potential, we allow for a nontrivial dependence of the cubic Horndeski function on the canonical kinetic term. This kinetic structure modifies the effective friction acting on the inflaton and the dynamics of curvature perturbations, enabling a transient ultra-slow-roll phase without the need for sharp potential features. As a result, the growth and localization of the peak in the curvature power spectrum can be efficiently controlled, leading to PBH production in mass ranges consistent with current observational constraints. In particular, we demonstrate that PBHs with asteroid-scale masses can form and constitute a substantial fraction of the present dark matter abundance within this framework.

The paper is organised as follows. In Sec. II, we introduce the Horndeski gravity setup considered in this work. In Sec. III, we analyse the realization of ultra-slow-roll inflation, discussing separately the background dynamics and scalar perturbations. In Sec. IV, we study the resulting curvature power spectrum and the correspond-

ing primordial black hole abundance. Finally, Sec. V is devoted to our conclusions.

II. THE FUNDAMENTALS OF HORNDESKI GRAVITY AND COSMOLOGY

In this section we briefly review Horndeski gravity. The action of the theory has the following form: [35–37]

$$S = \int d^4x \sqrt{-g} (\mathcal{L} + \mathcal{L}_m), \quad (1)$$

where

$$\mathcal{L} = \sum_{i=2}^5 \mathcal{L}_i, \quad (2)$$

with

$$\mathcal{L}_2 = K(\phi, X), \quad (3)$$

$$\mathcal{L}_3 = -G_3(\phi, X) \square \phi, \quad (4)$$

$$\mathcal{L}_4 = G_4(\phi, X) R + G_{4,X} [(\square \phi)^2 - (\nabla_\mu \nabla_\nu \phi) (\nabla^\mu \nabla^\nu \phi)], \quad (5)$$

$$\begin{aligned} \mathcal{L}_5 = & G_5(\phi, X) G_{\mu\nu} (\nabla^\mu \nabla^\nu \phi) \\ & - \frac{1}{6} G_{5,X} [(\square \phi)^3 - 3(\square \phi) (\nabla_\mu \nabla_\nu \phi) (\nabla^\mu \nabla^\nu \phi) \\ & + 2(\nabla^\mu \nabla_\alpha \phi) (\nabla^\alpha \nabla_\beta \phi) (\nabla^\beta \nabla_\mu \phi)], \end{aligned} \quad (6)$$

where \mathcal{L}_m stands for the Lagrangian describing the matter content of the universe. In the expressions for \mathcal{L}_i , $X \equiv -\frac{1}{2} g^{\mu\nu} \partial_\mu \phi \partial_\nu \phi$ denotes the canonical kinetic term, R the Ricci scalar and $G_{\mu\nu}$ the Einstein tensor. Furthermore, the function $K(\phi, X)$ embodies a generalization of the scalar energy contribution, while $G_3(\phi, X)$ can be viewed as a generalized derivative ϕ -dependent coupling between the metric tensor and the second-order derivatives of ϕ , inducing a scalar-metric kinetic mixing known as kinetic gravity braiding. Additionally, G_4 is a generalized $G_{5,X}$ terms respectively introduce quartic and quintic interactions of ϕ due to the kinetic dependence of G_4 and G_5 .

In order to apply Horndeski gravity at a cosmological framework, we introduce the flat Friedmann-Lemaître-Robertson-Walker (FLRW) metric

$$ds^2 = -dt^2 + a^2(t)(dx^2 + dy^2 + dz^2), \quad (7)$$

where $a(t)$ is the scale factor. Hence, in this case the scalar field will be just a function of the cosmic time, namely $\phi(t)$, while its kinetic energy becomes $X = \dot{\phi}^2/2$.

As we mentioned in the Introduction, in the present work we are interested in Horndeski subclasses that are consistent with GW170817 observations. Since the gravitational-wave speed in Horndeski theories around an FLRW background is in general different than 1, and it is given by [69]

$$c_T^2 \equiv \frac{2G_4 - 2XG_{5,\phi} - 2XG_{5,X}\ddot{\phi}}{2(G_4 - 2XG_{4,X}) - 2X(G_{5,X}\dot{\phi}H - G_{5,\phi})} \geq 0, \quad (8)$$

we can see that excluding G_{4X} and G_5 contributions immediately ensures viability against GW170817 constraints. Thus, the action of our theory remains as

$$S = \int d^4x \sqrt{-g} [K(\phi, X) - G_3(\phi, X) \square \phi + G_4(\phi) R]. \quad (9)$$

We choose $G_4 = M_{\text{Pl}}^2/2$ to directly recover the Einstein-Hilbert term, and consider the standard form for the function K which is $K = X - V(\phi)$, where $V(\phi)$ is the scalar potential. We observe that this choice retains the canonical kinetic term and standard slow-roll behavior in the limit $G_3 \rightarrow 0$, allowing at the same time for effects of kinetic self-interactions to be systematically studied through the function $G_3(\phi, X)$.

Working at the background level, one can extract the respective Friedmann and Klein-Gordon equations for the dynamical evolution of the scale factor and the scalar field ϕ by minimising respectively the action (9) with respect to the metric $g_{\mu\nu}$ and the scalar field ϕ . In particular, the Friedmann equations in Planck units read as [35–37]

$$3H^2 = V + \frac{\dot{\phi}^2}{2} + \dot{\phi}^2(3H\dot{\phi}G_{3X} - G_{3\phi}), \quad (10)$$

$$2\dot{H} + 3H^2 = V - \frac{\dot{\phi}^2}{2} \left[1 - 2(\ddot{\phi}G_{3X} + G_{3\phi}) \right], \quad (11)$$

where $H \equiv \dot{a}/a$ is the Hubble function. Additionally, the ϕ -evolution equation is extracted as

$$\ddot{\phi} + 3H\dot{\phi} \left(\frac{\mathcal{A}}{\mathcal{B}} \right) + \frac{\mathcal{C}}{\mathcal{B}} = 0, \quad (12)$$

with

$$\begin{aligned} \mathcal{A} &= 1 + H\dot{\phi}G_{3X}[3 - \epsilon] - 2G_{3\phi} + \dot{\phi}^2G_{3\phi X} \\ \mathcal{B} &= V\phi - \dot{\phi}^2G_{3\phi\phi} \\ \mathcal{C} &= 1 + 6H\dot{\phi}G_{3X} - 2G_{3\phi} + 3H\dot{\phi}^3G_{3XX} - \dot{\phi}^2G_{3\phi X}. \end{aligned} \quad (13)$$

We proceed by examining the linear scalar perturbations. Working in the unitary gauge, namely setting $\delta\phi = 0$, we perturb the spatial part of the metric as $\gamma_{ij} = a^2(t)e^{2\zeta}(e^h)_{ij}$, where ζ is the curvature perturbation and h_{ij} the tensor perturbation [37, 69, 70]. The importance of the curvature perturbation ζ lies in the fact that, on super-horizon scales, ζ is conserved [71] and, thus, it can be used to propagate intact the inflationary power spectrum from the end of inflation onwards. To extract then the equation of motion of the scalar curvature perturbation we need to derive the quadratic action in ζ , ultimately recast as [37]

$$S^{(2)} = \int dt d^3x a^3 \left(\mathcal{G}_s \dot{\zeta}^2 - \frac{\mathcal{F}_s}{a^2} (\nabla \zeta)^2 \right), \quad (14)$$

where \mathcal{G}_s , \mathcal{F}_s are given in the Appendix. Working in terms of the conformal time η defined as $d\eta = dt/a$ and

introducing a new curvature perturbation variable, usually called Mukhanov-Sasaki (MS) variable u , defined as $u \equiv z_s \zeta$ where $z_s = \sqrt{2\mathcal{G}_s} a$, one can write Eq. (14) as

$$S^{(2)} = \frac{1}{2} \int d\eta d^3x \left(u'^2 - c_s^2 (\nabla u)^2 + \frac{z_s''}{z_s} u^2 \right), \quad (15)$$

where $c_s = \mathcal{F}_s/\mathcal{G}_s$ is the sound speed. Hence, by minimising (15) one extracts the equation of motion for the MS variable, reading as

$$u_k'' + \left(c_s^2 k^2 - \frac{z_s''}{z_s} \right) u_k = 0. \quad (16)$$

Moreover, in terms of the e-fold number defined as $N \equiv \ln a$ Eq. (16) can be recast as

$$u_k'' + \left(1 + \frac{H'}{H} \right) u_k' + \left\{ \frac{c_s^2 k^2}{a^2 H^2} - \frac{1}{z_s} \left[z_s'' + \left(1 + \frac{H'}{H} \right) z_s' \right] \right\} u_k = 0, \quad (17)$$

where H is the usual (cosmic-time) Hubble function, primes now denote derivatives with respect to N , and the quantities $\frac{z_s'}{z_s}$ and $\frac{z_s''}{z_s}$ read as

$$\begin{aligned} \frac{z_s'}{z_s} &= 1 + \frac{1}{2} \frac{\mathcal{G}_s'}{\mathcal{G}_s} \\ \frac{z_s''}{z_s} &= \frac{1}{2} \frac{\mathcal{G}_s''}{\mathcal{G}_s} + \frac{\mathcal{G}_s'}{\mathcal{G}_s} + 1 - \frac{1}{4} \left(\frac{\mathcal{G}_s'}{\mathcal{G}_s} \right)^2. \end{aligned} \quad (18)$$

III. ULTRA-SLOW ROLL INFLATION IN HORNDESKI GRAVITY

In this section we investigate how ultra-slow-roll inflation can be realized within the GW170817-compatible Horndeski framework introduced above. We analyze separately the background dynamics and the evolution of scalar perturbations, emphasizing the role of the cubic Horndeski interaction in inducing a transient enhancement of friction without introducing peculiar features in the inflationary potential.

A. Background dynamics and enhanced friction

Focusing now on an inflationary realization within our Horndeski gravity framework, we introduce the first Hubble-flow slow-roll parameter ϵ , defined as

$$\epsilon \equiv -\frac{\dot{H}}{H^2}. \quad (19)$$

Making use of the Friedmann equation (10), one can show that ϵ takes the form

$$\epsilon = \frac{\dot{\phi}^2}{2H^2} \left[1 - G_{3X}(\ddot{\phi} - 3H\dot{\phi}) - 2G_{3\phi} \right]. \quad (20)$$

In what follows, we decompose for simplicity the cubic Galileon function as

$$G_3(\phi, X) = f(\phi) g(X). \quad (21)$$

In order to realize a standard slowly varying phase, namely with $\dot{\phi} = \sqrt{2X}$ remaining small, we exclude X -dependences of the type $1/\dot{\phi}^n$ with $n \geq 1$, since these X -dependences would render the $\dot{\phi}$ -dependent terms in Eqs. (10)-(12) excessively large, leading to a breakdown of the slow-roll regime.

Furthermore, since the ultra-slow-roll (USR) phase is expected to occur when X becomes very small, we also avoid monotonic dependences such as $\dot{\phi}$, $\ln \dot{\phi}$, or $1/\dot{\phi}^n$ with $n < 1$, which would suppress the contribution of G_3 and prevent any enhanced friction from developing. Exploiting instead the smallness of X during USR, we adopt an exponential dependence

$$g(X) = Ae^{-nX}, \quad (22)$$

where A and $n > 0$ are constants. This choice allows the system to remain in a standard slow-roll phase while enabling a transient enhancement of the G_3 contribution when X becomes sufficiently small.

Under the assumptions $|\epsilon|, |\eta|, |\beta| \ll 1$, with

$$\eta = -\frac{\ddot{\phi}}{H\dot{\phi}}, \quad \beta = \frac{\dot{\phi}^2 G_{3\phi\phi}}{V_\phi}, \quad (23)$$

slow-roll inflation is governed by the approximate Friedmann equations

$$3H^2 \simeq V, \quad (24)$$

$$3H\dot{\phi}(1 + D_1 + D_2) + V_\phi \simeq 0, \quad (25)$$

$$\epsilon \simeq \frac{\dot{\phi}^2}{2H^2}(1 + D_1 + D_2), \quad (26)$$

where

$$D_1(\phi, X) = -3nAH\dot{\phi}fe^{-nX} = 3H\dot{\phi}G_{3X}, \\ D_2(\phi, X) = -2Af_\phi e^{-nX} = -2G_{3\phi}. \quad (27)$$

In practice, we will assume $D_1 \ll D_2$, which simplifies the analysis without affecting the qualitative behavior. Having extracted above the Friedmann, the Klein-Gordon equations and the first slow-roll parameter in the slow-roll regime, one can compute the power spectrum of the curvature perturbation ζ [37]. After a straightforward calculation, one gets that during the slow-roll phase

$$\mathcal{P}_\zeta \simeq \frac{H^4}{4\pi^2 \dot{\phi}^2 (1 + D_2)} \simeq \frac{V^3}{12\pi^2 V_\phi^2} (1 + D_2), \quad (28)$$

while the power spectrum of first-order tensor perturbations remains unchanged, that is, $P_T = 2H^2/\pi^2 \simeq 2V/3\pi^2$. Following this, the scalar spectral index and

the tensor-to-scalar ratio will be given by the following approximated expressions:

$$n_S - 1 \simeq \frac{2}{1 + D_2} \left(\eta_V - 3\epsilon_V + \frac{D_{2\phi}}{1 + D_2} \sqrt{\frac{\epsilon_V}{2}} \right), \\ r \simeq \frac{16\epsilon_V}{1 + D_2}, \quad (29)$$

where $\epsilon_V = (V'/V)^2/2$ and $\eta_V = V''/V$ are the potential slow-roll parameters.

While the kinetic dependence of G_3 determines the enhancement of friction, the onset and exit of the USR phase, as well as its localization toward the end of inflation, are controlled by the ϕ -dependence of $f(\phi)$. To this end, motivated by its relation with the power spectrum in expression (29), we choose

$$f(\phi) = -BC \sinh^{-1} \left[\frac{\phi - \phi_c}{C} \right], \quad (30)$$

which leads to a Lorentzian-type localized profile of its derivative f_ϕ , where B and C are constants and ϕ_c denotes the field value at which the USR phase is triggered. The parameter B controls the amplitude of the friction enhancement, while C regulates the duration of the USR phase in terms of e-folds. This f form ensures a smooth entrance into, and exit from, the USR regime.

The mechanism described above can operate for a broad class of inflationary potentials. For concreteness, we adopt a logarithmic potential

$$V(\phi) = V_0 \ln(\alpha + \gamma\phi^\delta), \quad (31)$$

with $\alpha, \gamma > 0$ and $\delta > 0$, ensuring that the potential is smooth and positive for $\phi > 0$. This form interpolates between monomial and plateau-like behavior and may arise in effective descriptions of high-energy or string-inspired scenarios [61, 72, 73]. In the following, we fix $\alpha = \gamma = \delta = 1$ in Planck units for simplicity, and we restrict to $\phi > 0$, corresponding to the dynamically relevant inflationary region.

Fixing V_0 to match CMB observations at $k_{\text{CMB}} = 0.05 \text{ Mpc}^{-1}$ and $\phi_{\text{in}} = 6.2$, we obtain $\mathcal{P}_\zeta \simeq 2.1 \times 10^{-9}$, $n_s = 0.9673$, and $r = 0.038$. Achieving the enhancement necessary for PBH formation on small scales requires $A \cdot B = \mathcal{O}(10^8)$, with C chosen sufficiently small to control the USR duration. In what follows, we adopt $A = 10^3$ and $n = 1$ as representative values.

B. Scalar perturbations and power spectrum enhancement

During the ultra-slow-roll phase, slow-roll conditions are violated by construction, and the approximate expressions derived above cease to be valid. In this regime, the dynamics of scalar perturbations must be obtained by solving the MS equation, which we solve numerically, using Eqs. (24)-(26) with $D_1 \ll D_2$ as initial conditions.

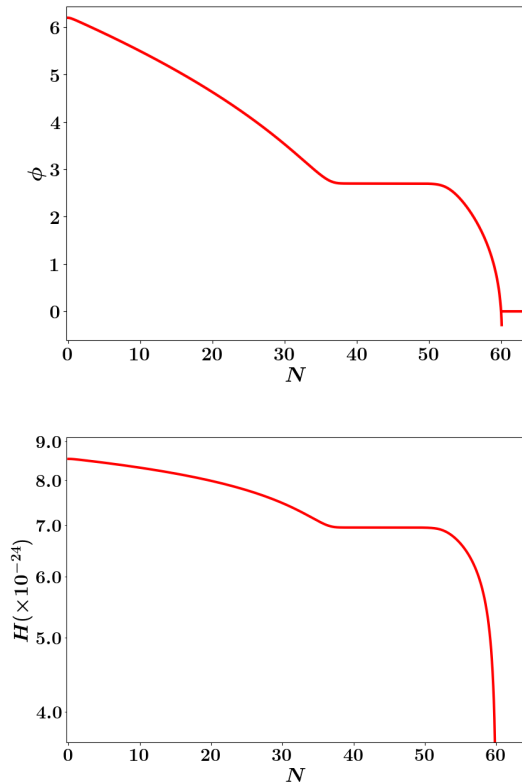


FIG. 1: Evolution of the field ϕ and the Hubble parameter H with respect to the e -fold number N , for the case (a) of Table I.

For the MS variable u_k and its conformal-time derivative u'_k , we impose Bunch-Davies initial conditions deep inside the horizon ($-k\eta \rightarrow \infty$),

$$u_k = \frac{1}{\sqrt{2c_s k}}, \quad u'_k = -i\sqrt{\frac{c_s k}{2}}, \quad (32)$$

where c_s denotes the effective sound speed.

We present two representative parameter choices, namely cases (a) and (b), in Table I, which lead to qualitatively different PBH spectra. For both cases, quantities \mathcal{F}_s and \mathcal{G}_s remain positive, so there are no ghost or gradient instabilities, and additionally there exist viable configurations. In Figs. 1, 2, 3 we show the background evolution and the scalar power spectrum for case (a). The USR phase occurs around $N \simeq 35$ -50 e -folds, while standard slow-roll inflation is recovered outside this interval and ends at $N \simeq 59$.

As we observe, the rapid suppression of $\dot{\phi}$ during USR is reflected in the deepening of the slow-roll parameter ϵ and the sharp variation of η , signaling the importance of $\dot{\phi}$ in this regime. The resulting scalar power spectrum exhibits a pronounced peak at small scales around $k \simeq 10^{14} \text{ Mpc}^{-1}$, while remaining nearly scale-invariant on CMB scales. The spectrum satisfies current constraints from PTA observations, BBN, and CMB μ -

distortions.

The location and height of the peak are sensitive to the model parameters at the level of the second decimal place, corresponding to moderate fine tuning. The small oscillations following the peak arise from cumulative $\dot{\phi}$ -dependent effects induced by the kinetic structure of $G_3(X)$, which are absent in more conventional treatments. The pronounced oscillations in the power spectrum arise from the sharp, non-adiabatic nature of the transition into the USR phase. Modes on the left of the peak ($k < k_{\text{peak}}$) exited the horizon prior to this transition; having already frozen out, they remain unaffected and smooth. Conversely, modes on the right ($k > k_{\text{peak}}$) were still deep inside the horizon during the transition. These sub-horizon modes experienced the sharp change in the background dynamics while oscillating, inducing phase shifts that result in the observed constructive and destructive interference pattern. In case (b), which is also shown in Fig. 3, the earlier transition intercepts larger modes during their horizon exit, extending the oscillations to the left of the peak.

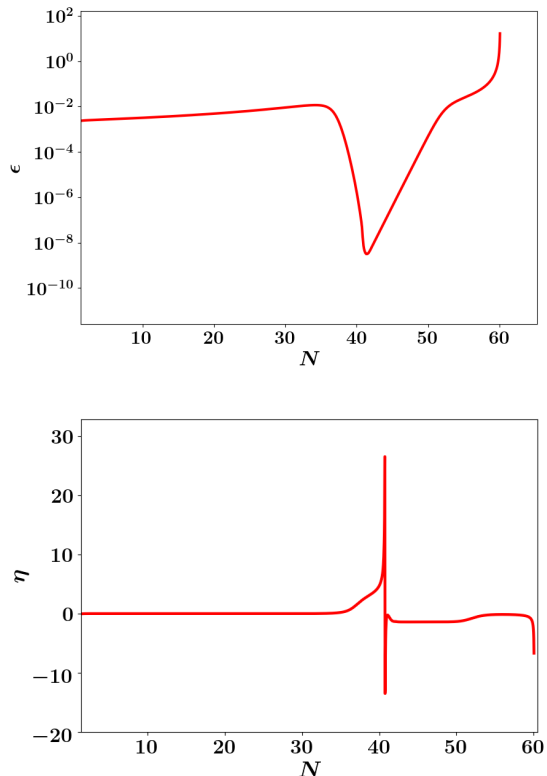


FIG. 2: Evolution of the first (ϵ) and second (η) slow-roll parameters with respect to the e -fold number N , for the case (a) of Table I.

TABLE I: Representative parameter values yielding an enhancement of the scalar power spectrum consistent with observational constraints and leading to primordial black hole (PBH) production. All dimensional quantities are expressed in Planck units.

Case	V_0	ϕ_c	B	C	n_s	$k_{\text{peak}}(\text{Mpc}^{-1})$	$P_{\zeta, \text{peak}}$	M_{PBH}/M_\odot	f_{PBH}
(a)	0.656×10^{-9}	2.7	3.84×10^5	1.52×10^{-10}	0.9673	1.51×10^{14}	1.16×10^{-2}	1.04×10^{-16}	0.92
(b)	1.9×10^{-9}	4.82	2.09×10^5	1.4×10^{-10}	0.9690	6.45×10^7 & 1.41×10^7 (secondary)	1.62×10^{-2} & 1.62×10^{-2} (sec.)	6.35×10^{-4} & 1.26×10^{-2} (sec.)	8.68×10^{-3} & 1.78×10^{-3} (sec.)

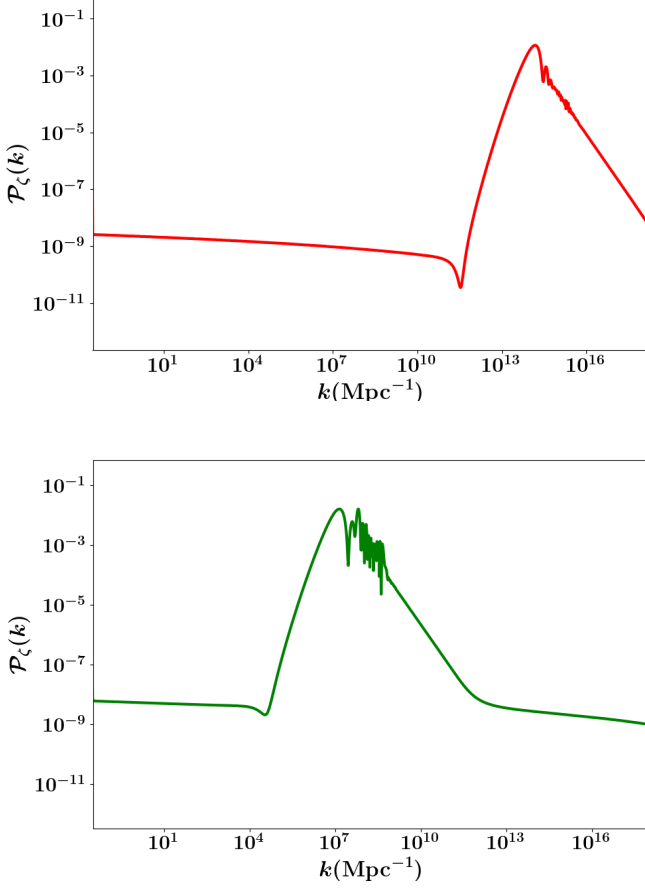


FIG. 3: Profile of the scalar power spectrum \mathcal{P}_ζ as a function of the comoving wavenumber k , for the case (a) (red color) and (b) (green color) of Table I.

IV. PRIMORDIAL BLACK HOLE PRODUCTION

Let us now study the formation of primordial black holes in the present framework. In order to do that we adopt the standard Press-Schechter-based approach [74]. We parameterize the fraction of the horizon mass that collapses into a black hole at formation by γ , and we fix $\gamma = 0.36$ according to recent simulations [75]. Given the observationally inferred dark matter density $\Omega_{\text{DM}} h^2 = 0.12$, the present-day fraction of dark matter composed of PBHs with mass M is given by [8]

$$f_{\text{PBH}}(M) = \frac{\beta(M)}{3.94 \times 10^{-9}} \left(\frac{g_*}{10.75} \right)^{-1/4} \left(\frac{M}{M_\odot} \right)^{-1/2}, \quad (33)$$

where g_* denotes the effective number of relativistic degrees of freedom at PBH formation, M_\odot is the solar mass, and $\beta(M)$ is the fraction of the Universe's energy density collapsing into PBHs of mass M at horizon re-entry.

The quantity $\beta(M)$ is determined by the statistics of the primordial density perturbations. Assuming Gaussian fluctuations, $\beta(M)$ can be estimated from the tail of the probability distribution of the coarse-grained density contrast. This probability depends on the variance $\sigma(M)$ of density perturbations smoothed on the scale associated with the mass M , and on the critical density threshold δ_c required for gravitational collapse to overcome pressure and cosmic expansion. Working within the Press-Schechter formalism, $\beta(M)$ will read as

$$\beta(M) \equiv 2 \int_{\delta_c}^{\infty} \text{PDF}(\delta) d\delta = 2 \int_{\delta_c}^{\infty} \frac{1}{\sqrt{2\pi} \sigma(M)} e^{-\frac{\delta^2}{2\sigma^2(M)}} d\delta, \quad (34)$$

where the factor of 2 accounts for locally under threshold regions collapsing in globally over threshold regions in order to avoid double-counting PBHs. $\sigma^2(k)$ stands for the coarse-grained variance smoothed on a scale equal to the comoving horizon scale $R = (aH)^{-1}$, which at horizon-crossing time is equal to $R = k^{-1}$. For a radiation-dominated era, one has that [76, 77]

$$\sigma^2(k) = \frac{16}{81} \int_0^\infty \frac{dk}{k} (kR)^4 \tilde{W}^2(k, R) \mathcal{P}_\zeta(k), \quad (35)$$

where $W(\vec{x}, R)$ denotes the window function, chosen to be a Gaussian one, whose Fourier transform reads as [78]

$$\tilde{W}(k, R) = e^{-k^2 R^2/2}. \quad (36)$$

Assuming high peaked collapsing regions, i.e. $\delta_c > \sigma$, which is a good approximation for our case, as it was checked numerically, $\beta(M)$ can be recast as

$$\beta(M) = \sqrt{\frac{2}{\pi}} \frac{\sigma(k)}{\delta_c} \exp\left(-\frac{\delta_c^2}{2\sigma^2(k)}\right), \quad (37)$$

where for a radiation-dominated era, we adopt $\delta_c = 0.4$ [79] following recent simulations on PBH formation.

Assuming a scale-invariant power spectrum as a first approximation, we get $\sigma(k) \simeq \frac{4}{9} \sqrt{P_\zeta}$, so

$$\beta(M) \simeq \sqrt{\frac{2}{\pi}} \frac{\sqrt{P_\zeta}}{\mu_c} \exp\left(-\frac{\mu_c^2}{2P_\zeta}\right), \quad (38)$$

where $\mu_c = 9\delta_c/4$, and P_ζ denotes the curvature power spectrum evaluated at the scale corresponding to M .

Additionally, the PBH mass associated with a comoving wavenumber k is given by

$$M(k) = 3.68 \left(\frac{g_*}{10.75} \right)^{-1/6} \left(\frac{k}{10^6 \text{ Mpc}^{-1}} \right)^{-2} M_\odot \quad (39)$$

In the present analysis we take $g_* = 106.75$, appropriate for temperatures $T \gtrsim 300 \text{ GeV}$. From the above expression, we can explicitly see the mapping between the comoving scale k and the PBH mass M .

For the curvature power spectra and the peak scales reported in Table I, Eqs. (33), (38) and (39) yield the PBH abundances shown in Fig. 4. As we can see, the resulting PBH mass spectrum can be broadly divided into distinct regimes. At sufficiently low masses, PBHs have already evaporated, or are evaporating today, due to Hawking radiation and are strongly constrained due to evaporation observational limits. On the other hand, at very large masses, PBHs correspond to intermediate or super-massive objects and can contribute only a subdominant fraction of the dark matter abundance due to observational constraints from microlensing [80], GWs [81] and CMB [82].

However, interestingly enough, in between these regimes lies a mass window where PBHs can constitute a substantial, or even dominant, component of dark matter while remaining consistent with current observational bounds, including white dwarf (WD) constraints [83, 84]. In particular, for the case (a) of Table I we obtain PBH masses of order of $M_{\text{PBH}} \sim 10^{-16} M_\odot$, corresponding to $M \sim 2 \times 10^{17} \text{ g}$, i.e. asteroid-mass PBHs. This mass range falls within the window where PBHs may account for essentially the entire dark matter abundance. In this case, the predicted PBH fraction reaches $f_{\text{PBH}} \simeq 0.93$, while satisfying existing WD constraints. We mention here that the enhanced scalar perturbations associated with the ultra-slow-roll phase are also expected to source scalar-induced gravitational waves (SIGWs) at second order in cosmological perturbation theory [85]. Given the peak scale $k_{\text{peak}} \simeq 10^{14} \text{ Mpc}^{-1}$, the corresponding GW peak frequency f can be recast as $f = k/(2\pi a_0) \sim 1 \text{ Hz}$, where we use that today a_0 is normalised to unity, lying in between the frequency detection bands of LISA and ET. and motivating thus future dedicated studies in connection with such GW detectors.

Case (b) leads to a different PBH mass scale and abundance, resulting to a smaller contribution to the total dark matter density. The intensified oscillatory behavior observed at larger mass scales modulates the power spectrum sufficiently to generate a secondary collapse window, resulting in a double-peaked PBH abundance. These examples illustrate how variations in the parameters controlling the ultra-slow-roll phase and the curvature power spectrum directly translate into distinct PBH phenomenology within the present framework.

Finally, we mention here that ultra-slow-roll phases are known to potentially generate sizable non-Gaussianities

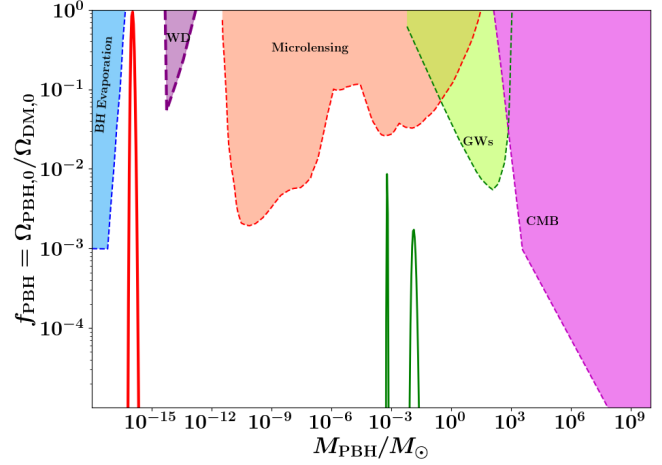


FIG. 4: The PBHs abundance f_{PBH} with respect to the PBHs masses M , on top of the observational constraints from CMB (pink color), GWs (green color), Microlensing (orange color), WD (purple color) and BH Evaporation (blue color), for the case (a) and case (b) of Table I. The asteroid-mass window, at roughly $10^{-11} - 10^{-16} M_\odot$, could account for 100% of DM.

in the curvature perturbations [20, 86, 87], which may affect primordial black hole abundance estimates based on Gaussian statistics. The quantitative impact of such effects depends sensitively on the detailed dynamics of the ultra-slow-roll phase and on the shape of the curvature power spectrum around its peak. A dedicated analysis of non-Gaussian corrections to the PBH abundance within the present Horndeski framework is beyond the scope of this work and is left for future investigation.

V. CONCLUSIONS

In this work we studied the production of primordial black holes within an inflationary scenario embedded in the Horndeski modified gravity framework, imposing two key physical requirements: the propagation speed of gravitational waves coincides with the speed of light at late times, as dictated by the GW170817 observation, and the coupling to the curvature scalar remains constant, corresponding to the standard Einstein-Hilbert term. Under these conditions, and retaining a canonical kinetic term as well as a smooth inflationary potential through $K(\phi, X)$, the inflationary dynamics and the enhancement of curvature perturbations are governed entirely by the cubic Horndeski contribution $G_3(\phi, X)$.

We showed that a suitable kinetic dependence of G_3 can induce a transient phase of ultra-slow-roll inflation by effectively enhancing the friction acting on the scalar field, without introducing features or discontinuities in the potential. Among standard classes of X -dependences, we found that an exponential dependence

is uniquely capable of preserving a conventional slow-roll phase, while generating a controlled ultra-slow-roll epoch. In this way, even a mild, localized ϕ -dependence in G_3 can be amplified into a pronounced peak in the curvature power spectrum, sufficient for primordial black hole formation, while remaining consistent with observational constraints from the CMB, pulsar timing arrays, big-bang nucleosynthesis, and CMB μ -distortions.

Applying this mechanism to a representative smooth plateau-type potential, here chosen in logarithmic form, we identified stable parameter configurations that lead to the formation of primordial black holes with masses of order $\mathcal{O}(10^{-16}) M_\odot$, corresponding to asteroid-mass PBHs. This mass range lies just above the threshold for complete Hawking evaporation at the present epoch and falls within a window where primordial black holes can constitute a substantial fraction of the dark matter abundance while satisfying existing observational bounds, including white dwarf constraints. In the examples presented, the resulting PBH abundance can reach values close to the total dark matter density, $f_{\text{PBH}} \simeq 0.9$. Additional viable solutions exist in the parameter space, leading to different PBH mass scales and abundances, illustrating the flexibility of the mechanism.

A notable feature of the present framework is that the required enhancement of the curvature power spectrum is achieved with relatively moderate parameter tuning compared to many alternative primordial black hole scenarios [88]. The key ingredient is the kinetic structure of the Horndeski interaction rather than a finely engineered inflationary potential or ϕ dependence, allowing the background inflationary predictions on CMB scales to remain essentially unchanged.

The results presented here open several directions for further investigation. A particularly important extension concerns the stochastic gravitational-wave background induced at second order by the enhanced scalar perturbations associated with the ultra-slow-roll phase [85]. Given the sharp peak in the curvature power spectrum and the oscillatory pattern on high- k regions, the corresponding scalar-induced GW signal is expected to exhibit characteristic spectral features, potentially falling within the sensitivity ranges of future detectors such as the LISA or the Einstein Telescope. A detailed analysis of this signal would provide an additional observational handle on the mechanism discussed here. Further studies could also address the role of non-Gaussianities generated during the ultra-slow-roll phase, as well as the embedding of the present scenario within more complete models of reheating and post-inflationary evolution. Together, these extensions would help clarify the observational viability of primordial black holes arising from modified-gravity-induced inflationary dynamics, and further elucidate the connection between early modified gravity and the present dark matter content of the Universe.

Acknowledgments

The authors gratefully acknowledge the contribution of the LISA Cosmology Working Group (CosWG), as well as support from the COST Actions CA21136 - Address-

ing observational tensions in cosmology with systematics and fundamental physics (CosmoVerse) - CA23130, Bridging high and low energies in search of quantum gravity (BridgeQG) and CA21106 - COSMIC WISPer in the Dark Universe: Theory, astrophysics and experiments (CosmicWISPer). TP acknowledges as well the support of the INFN Sezione di Napoli through the project QGSKY.

Appendix A: The coefficient functions of the quadratic action for scalar perturbations

In Horndeski gravity, the quadratic action for scalar perturbations around an FLRW background is given as [37]

$$S^{(2)} = \int dt d^3x a^3 \left(\mathcal{G}_s \dot{\zeta}^2 - \frac{\mathcal{F}_s}{a^2} (\nabla \zeta)^2 \right), \quad (\text{A1})$$

where ζ is the curvature perturbation. The coefficient functions are given by [70, 89]

$$\mathcal{F}_s \equiv \frac{1}{a} \frac{d\xi}{dt} - \mathcal{F}_T, \quad (\text{A2})$$

$$\mathcal{G}_s \equiv \frac{\Sigma}{\Theta^2} \mathcal{G}_T^2 + 3\mathcal{G}_T, \quad (\text{A3})$$

where

$$\mathcal{F}_T \equiv 2 \left[G_4 - X \left(\ddot{\phi} G_{5,X} + G_{5,\phi} \right) \right], \quad (\text{A4})$$

$$\mathcal{G}_T \equiv 2 \left[G_4 - 2XG_{4,X} - X \left(H\dot{\phi} G_{5,X} - G_{5,\phi} \right) \right], \quad (\text{A5})$$

with

$$\xi \equiv \frac{a\mathcal{G}_T^2}{\Theta}, \quad (\text{A6})$$

and

$$\begin{aligned} \Sigma \equiv & XK_{,X} + 2X^2 K_{,XX} + 12H\dot{\phi} X G_{3,X} \\ & + 6H\dot{\phi} X^2 G_{3,XX} - 2XG_{3,\phi} - 2X^2 G_{3,\phi X} - 6H^2 G_4 \\ & + 6 \left[H^2 (7XG_{4,X} + 16X^2 G_{4,XX} + 4X^3 G_{4,XXX}) \right. \\ & \quad \left. - H\dot{\phi} (G_{4,\phi} + 5XG_{4,\phi X} + 2X^2 G_{4,\phi XX}) \right] \\ & + 30H^3 \dot{\phi} X G_{5,X} + 26H^3 \dot{\phi} X^2 G_{5,XX} \\ & - 6H^2 X (6G_{5,\phi} + 9XG_{5,\phi X} + 2X^2 G_{5,\phi XX}) \\ & + 4H^3 \dot{\phi} X^3 G_{5,XXX}, \end{aligned} \quad (\text{A7})$$

$$\begin{aligned} \Theta \equiv & -\dot{\phi} X G_{3,X} + 2H G_4 - 8H X G_{4,X} \\ & - 8H X^2 G_{4,XX} + \dot{\phi} G_{4,\phi} + 2X\dot{\phi} G_{4,\phi X} \\ & - H^2 \dot{\phi} (5XG_{5,X} + 2X^2 G_{5,XX}) \\ & + 2H X (3G_{5,\phi} + 2XG_{5,\phi X}). \end{aligned} \quad (\text{A8})$$

-
- [1] N. Aghanim et al. (Planck) (2018), 1807.06209.
 - [2] G. Bertone, D. Hooper, and J. Silk, Phys. Rept. **405**, 279 (2005), hep-ph/0404175.
 - [3] J. L. Feng, Ann. Rev. Astron. Astrophys. **48**, 495 (2010), 1003.0904.
 - [4] Y. B. Zel'dovich and I. D. Novikov, Sov. Astron. **10**, 602 (1967).
 - [5] S. Hawking, Mon. Not. Roy. Astron. Soc. **152**, 75 (1971).
 - [6] B. J. Carr and S. W. Hawking, Mon. Not. Roy. Astron. Soc. **168**, 399 (1974).
 - [7] M. Sasaki, T. Suyama, T. Tanaka, and S. Yokoyama, Class. Quant. Grav. **35**, 063001 (2018), 1801.05235.
 - [8] B. Carr, K. Kohri, Y. Sendouda, and J. Yokoyama, Rept. Prog. Phys. **84**, 116902 (2021), 2002.12778.
 - [9] A. M. Green and B. J. Kavanagh, J. Phys. G **48**, 043001 (2021), 2007.10722.
 - [10] A. Escrivà, F. Kuhnel, and Y. Tada (2022), 2211.05767.
 - [11] P. Ivanov, P. Naselsky, and I. Novikov, Phys. Rev. D **50**, 7173 (1994).
 - [12] K. Inomata, M. Kawasaki, K. Mukaida, Y. Tada, and T. T. Yanagida, Phys. Rev. D **96**, 043504 (2017), 1701.02544.
 - [13] S. S. Mishra and V. Sahni, JCAP **04**, 007 (2020), 1911.00057.
 - [14] O. Özsoy, S. Parameswaran, G. Tasinato, and I. Zavala (2018), 1803.07626.
 - [15] S. Heydari and K. Karami, JCAP **02**, 047 (2024), 2309.01239.
 - [16] J. Garcia-Bellido, A. D. Linde, and D. Wands, Phys. Rev. D **54**, 6040 (1996), astro-ph/9605094.
 - [17] S. Clesse and J. García-Bellido, Phys. Rev. D **92**, 023524 (2015), 1501.07565.
 - [18] N. C. Tsamis and R. P. Woodard, Phys. Rev. D **69**, 084005 (2004), astro-ph/0307463.
 - [19] W. H. Kinney, Phys. Rev. D **72**, 023515 (2005), gr-qc/0503017.
 - [20] J. Martin, H. Motohashi, and T. Suyama, Phys. Rev. D **87**, 023514 (2013), 1211.0083.
 - [21] J. Garcia-Bellido and E. Ruiz Morales (2017), 1702.03901.
 - [22] C. Germani and T. Prokopec (2017), 1706.04226.
 - [23] H. Motohashi and W. Hu (2017), 1706.06784.
 - [24] A. Y. Kamenshchik, A. Tronconi, T. Vardanyan, and G. Venturi, Phys. Rev. D **99**, 023528 (2019), 1812.02547.
 - [25] T. Papanikolaou, A. Lymperis, S. Lola, and E. N. Saridakis, JCAP **03**, 003 (2023), 2211.14900.
 - [26] S. Heydari and K. Karami, Eur. Phys. J. C **84**, 127 (2024), 2310.11030.
 - [27] A. E. Romano and S. A. Severino, Phys. Rev. D **94**, 043513 (2016), 1606.02377.
 - [28] K. Dimopoulos, Phys. Lett. **B775**, 262 (2017), 1707.05644.
 - [29] E. N. Saridakis et al. (CANTATA), *Modified Gravity and Cosmology. An Update by the CANTATA Network* (Springer, 2021), ISBN 978-3-030-83715-0, 2105.12582.
 - [30] T. Clifton, P. G. Ferreira, A. Padilla, and C. Skordis, Phys. Rept. **513**, 1 (2012), 1106.2476.
 - [31] S. Nojiri and S. D. Odintsov, Phys. Rept. **505**, 59 (2011), 1011.0544.
 - [32] S. Capozziello and M. De Laurentis, Phys. Rept. **509**, 167 (2011), 1108.6266.
 - [33] Y.-F. Cai, S. Capozziello, M. De Laurentis, and E. N. Saridakis, Rept. Prog. Phys. **79**, 106901 (2016), 1511.07586.
 - [34] E. Di Valentino et al. (CosmoVerse Network), Phys. Dark Univ. **49**, 101965 (2025), 2504.01669.
 - [35] G. W. Horndeski, Int. J. Theor. Phys. **10**, 363 (1974).
 - [36] C. Deffayet, X. Gao, D. A. Steer, and G. Zahariade, Phys. Rev. D **84**, 064039 (2011), 1103.3260.
 - [37] T. Kobayashi, M. Yamaguchi, and J. Yokoyama, Prog. Theor. Phys. **126**, 511 (2011), 1105.5723.
 - [38] C. Deffayet and D. A. Steer, Class. Quant. Grav. **30**, 214006 (2013), 1307.2450.
 - [39] R. Kase and S. Tsujikawa, Phys. Rev. D **90**, 044073 (2014), 1407.0794.
 - [40] S. Tsujikawa, JCAP **04**, 043 (2015), 1412.6210.
 - [41] F. Arroja, N. Bartolo, P. Karmakar, and S. Matarrese, JCAP **04**, 042 (2016), 1512.09374.
 - [42] E. Bellini, A. J. Cuesta, R. Jimenez, and L. Verde, JCAP **02**, 053 (2016), [Erratum: JCAP **06**, E01 (2016)], 1509.07816.
 - [43] A. De Felice, K. Koyama, and S. Tsujikawa, JCAP **05**, 058 (2015), 1503.06539.
 - [44] E. Babichev, C. Charmousis, and A. Lehébel, Class. Quant. Grav. **33**, 154002 (2016), 1604.06402.
 - [45] J. Ben Achour, D. Langlois, and K. Noui, Phys. Rev. D **93**, 124005 (2016), 1602.08398.
 - [46] L. Pogosian and A. Silvestri, Phys. Rev. D **94**, 104014 (2016), 1606.05339.
 - [47] F. Arroja, T. Okumura, N. Bartolo, P. Karmakar, and S. Matarrese, JCAP **05**, 050 (2018), 1708.01850.
 - [48] A. Ijjas, JCAP **02**, 007 (2018), 1710.05990.
 - [49] S. Capozziello, K. F. Dialektopoulos, and S. V. Sushkov, Eur. Phys. J. C **78**, 447 (2018), 1803.01429.
 - [50] N. Frusciante, S. Peirone, S. Casas, and N. A. Lima, Phys. Rev. D **99**, 063538 (2019), 1810.10521.
 - [51] N. Franchini and T. P. Sotiriou, Phys. Rev. D **101**, 064068 (2020), 1903.05427.
 - [52] L. Heisenberg, M. Bartelmann, R. Brandenberger, and A. Refregier, Phys. Rev. D **99**, 124020 (2019), 1902.03939.
 - [53] K. Destounis, R. D. B. Fontana, F. C. Mena, and E. Papantonopoulos, JHEP **10**, 280 (2019), 1908.09842.
 - [54] A. Ilyas, M. Zhu, Y. Zheng, Y.-F. Cai, and E. N. Saridakis, JCAP **09**, 002 (2020), 2002.08269.
 - [55] V. K. Oikonomou and F. P. Fronimos, Class. Quant. Grav. **38**, 035013 (2021), 2006.05512.
 - [56] K. F. Dialektopoulos, J. L. Said, and Z. Oikonomopoulou, Eur. Phys. J. C **82**, 259 (2022), 2112.15045.
 - [57] M. Petronikolou, S. Basilakos, and E. N. Saridakis, Phys. Rev. D **106**, 124051 (2022), 2110.01338.
 - [58] K. Takahashi, M. Minamitsuji, and H. Motohashi, PTEP **2023**, 013E01 (2023), 2209.02176.
 - [59] G. W. Horndeski and A. Silvestri, Int. J. Theor. Phys. **63**, 38 (2024), 2402.07538.
 - [60] C. Fu, P. Wu, and H. Yu, Phys. Rev. D **100**, 063532 (2019), 1907.05042.
 - [61] I. Dalianis, A. Kehagias, and G. Tringas, JCAP **01**, 037 (2019), 1805.09483.
 - [62] J. Lin, Q. Gao, Y. Gong, Y. Lu, C. Zhang, and F. Zhang, Phys. Rev. D **101**, 103515 (2020), 2001.05909.

- [63] B. P. Abbott et al. (LIGO Scientific, Virgo), Phys. Rev. Lett. **119**, 161101 (2017), 1710.05832.
- [64] P. Creminelli and F. Vernizzi, Phys. Rev. Lett. **119**, 251302 (2017), 1710.05877.
- [65] J. M. Ezquiaga and M. Zumalacárregui, Phys. Rev. Lett. **119**, 251304 (2017), 1710.05901.
- [66] Z. Yi, Y. Gong, B. Wang, and Z.-L. Wang, Phys. Rev. D **103**, 063534 (2021), 2007.09957.
- [67] F. Zhang, J. Lin, and Y. Ma, Phys. Rev. D **104**, 063526 (2021), 2106.10729.
- [68] C. Fu, P. Wu, and H. Yu, Phys. Rev. D **100**, 063532 (2019), 1907.05042.
- [69] A. De Felice and S. Tsujikawa, JCAP **02**, 007 (2012), 1110.3878.
- [70] S. Akama and T. Kobayashi, Phys. Rev. D **99**, 043522 (2019), 1810.01863.
- [71] D. Wands, K. A. Malik, D. H. Lyth, and A. R. Liddle, Phys. Rev. D **62**, 043527 (2000), astro-ph/0003278.
- [72] D. Baumann and L. McAllister, *Inflation and String Theory*, Cambridge Monographs on Mathematical Physics (Cambridge University Press, 2015), ISBN 978-1-107-08969-3, 978-1-316-23718-2, 1404.2601.
- [73] G. Ballesteros and C. Tamarit, JHEP **02**, 153 (2016), 1510.05669.
- [74] W. H. Press and P. Schechter, Astrophys. J. **187**, 425 (1974).
- [75] I. Musco, *Numerical Simulations of Primordial Black Holes* (2025).
- [76] V. De Luca, G. Franciolini, A. Kehagias, M. Peloso, A. Riotto, and C. Ünal, JCAP **07**, 048 (2019), 1904.00970.
- [77] S. Young, I. Musco, and C. T. Byrnes, JCAP **11**, 012 (2019), 1904.00984.
- [78] S. Young, C. T. Byrnes, and M. Sasaki, JCAP **1407**, 045 (2014), 1405.7023.
- [79] I. Musco, Phys. Rev. D **100**, 123524 (2019), 1809.02127.
- [80] H. Niikura et al., Nature Astron. **3**, 524 (2019), 1701.02151.
- [81] M. Sasaki, T. Suyama, T. Tanaka, and S. Yokoyama, Phys. Rev. Lett. **117**, 061101 (2016), [erratum: Phys. Rev. Lett. 121, no. 5, 059901 (2018)], 1603.08338.
- [82] Y. Ali-Haïmoud and M. Kamionkowski, Phys. Rev. D **95**, 043534 (2017), 1612.05644.
- [83] F. Capela, M. Pshirkov, and P. Tinyakov, Phys. Rev. D **87**, 123524 (2013), 1301.4984.
- [84] P. W. Graham, S. Rajendran, and J. Varela, Phys. Rev. D **92**, 063007 (2015), 1505.04444.
- [85] G. Domènech and A. Ganz, JCAP **01**, 020 (2025), 2406.19950.
- [86] V. Atal and C. Germani, Phys. Dark Univ. **24**, 100275 (2019), 1811.07857.
- [87] G. Ballesteros, J. Gambín Egea, T. Konstandin, A. Pérez Rodríguez, M. Pierre, and J. Rey (2024), 2412.14106.
- [88] P. S. Cole, A. D. Gow, C. T. Byrnes, and S. P. Patil, JCAP **08**, 031 (2023), 2304.01997.
- [89] T. Kobayashi, Phys. Rev. D **94**, 043511 (2016), 1606.05831.